Rigorous Analysis of Traveling Wave Photodetectors under High-Power Illumination

Damir Pasalic, *Student Member IEEE*, Rüdiger Vahldieck, *Fellow IEEE*, Andreas Aste*

Swiss Federal Institute of Technology Zurich, Laboratory for Electromagnetic Fields and Microwave Electronics, Gloriastr. 35, CH-8092 Zurich, Switzerland

*University of Basel, Institute of Physics, Klingelbergstr. 82, CH-4056, Switzerland

***Abstract* — An efficient hybrid method for the rigorous analysis of traveling-wave photodetectors (TWPDs) is presented. The method consists of a combination of the 2D drift-diffusion based semiconductor simulation in conjunction with a full-wave EM analysis of the overall structure. While the 2D simulation determines the conductivity profile of the semiconductor layers under illuminations of different optical power levels, the 3D simulation characterizes the corresponding RF performance of the TWPD. Comparison with available experimental data has shown excellent agreement.**

I. INTRODUCTION

High-power traveling-wave photodetectors (TWPDs) are key components in the design of modern broadband communication systems. The ability of the TWPDs to maintain high efficiency and broad bandwidth under high optical power illumination makes them important in microwave fiber optic links, especially as the optical amplification becomes more widely employed.

The TWPD is an *in-plane* illuminated device consisting of an optical and a microwave (MW) waveguide coupled together [3]. The optical waveguide is formed by transparent semiconductor cladding layers about the absorbing core. At the same time, the TWPD is a distributed structure that has an electrode arrangement designed to support traveling of RF waves with characteristic impedance matched to that of the external circuit. The bandwidth of the TWPD is not limited by the RC constant, but rather by optical and RF absorption constants and velocity mismatch between the optical and RF waves over the length of the TWPD. For high power handling capability of the TWPD, the modal optical absorption coefficient should be low [4].

Because of their importance, TWPDs have been widely investigated in the literature. However, all these studies have been done by means of an equivalent-circuit model of a *hybrid-coplanar* transmission line [3]. However, the equivalent model is not general enough because it is limited to the specific geometry of the TWPD. Furthermore, it is assumed that the semiconductor layers of the TWPD have a constant and uniform conductivity which is not entirely true. The charge carriers inside the semiconductors, governed by the drift and diffusion forces, will distribute themselves to satisfy the Poisson law and the boundary conditions. Accordingly the conductivity will change, affecting the microwave propagation characteristics. The optical signal applied at the input of the TWPD will further influence the conductivity distribution inside the semiconductors.

In this paper a method is presented for the rigorous analysis of TWPDs of general geometry. Since the interaction of TWPDs with the embedding planar microwave circuitry is of great importance to ensure maximum RF power transfer, for the first time S-parameter results are presented here as well. The analysis is done in two steps. First, a 2D semiconductor simulation of the structure is performed to obtain the carrier concentrations along the TWPD cross-section. In the second step, the conductivity distribution along the cross-section is calculated from the carrier concentrations and used in the 2D and 3D full-wave microwave simulations. Finally, the propagation characteristics of the RF wave and the S-parameters at the interface to the microwave circuit are obtained. For the full-wave EM simulation the FDTLM method [1], [2] has been employed.

II. THEORY

The electrons and holes in the semiconductor layer of the TWPD are acted upon by the drift and diffusion forces and are distributed to satisfy the applied bias as well as the boundary conditions at the surfaces of the structure and the heterojunction interfaces. The conductivity of the layers will change accordingly. Therefore, for an accurate analysis of a TWPD, a semiconductor simulation has to be performed to obtain the exact conductivity distribution along the TWPD cross section. Subsequently a full-wave simulation can be performed to obtain the microwave properties of the structure.

A. Semiconductor Analysis

The semiconductor analysis is based on the well known drift-diffusion model. The electron and hole concentrations as well as the electrostatic potential at the cross-section of the TWPD are obtained by solving Poisson, continuity and rate equations in the two dimensional simulation domain. The steady-state drift-diffusion equations are given by [6]:

$$\nabla\left(\varepsilon_0\varepsilon_r\cdot\nabla\varphi\right)=-q\cdot\left(p-n+N_D-N_A\right) \tag{1}$$

$$\nabla\cdot J_n=q\cdot R\left(\varphi,n,p\right)-q\cdot G_n \tag{2}$$

$$\nabla\cdot J_p=-q\cdot R\left(\varphi,n,p\right)+q\cdot G_p \tag{3}$$

$$J_n=q\mu_n n\cdot E+qD_n\cdot\nabla n \tag{4}$$

$$J_p=q\mu_p p\cdot E-qD_p\cdot\nabla p \tag{5}$$

where, φ is the electrostatic potential, n and p are the electron and hole carrier concentration, q is the unit charge, $N_{D,A}$ are the donor/acceptor concentrations, $J_{n,p}$ are the electron/hole currents, R is the carrier recombination rate, $G_{n,p}$ are electron/hole generation rate, while $\mu_{n,p}$ and $D_{n,p}$ are electron/hole mobilities and diffusivities, respectively. Two types of recombination are assumed in our model: Shockley-Read-Hall radiative and Auger recombination [6]. The optical generation rate is given by:

$$G_n=G_p=\frac{W_p}{hf}\cdot\alpha_{abs}\cdot\exp\left(-\frac{(x-x_0)^2}{\sigma_x^2}\right) \tag{6}$$

where W_p is the peak optical power density incident to the surface, hf is the photon energy, α_{abs} is the optical absorption coefficient, and x_0 is the center of the active region along the x-dimension. σ_x is related to the full width, half maximum (FWHM) of the optical beam along the x-direction. The beam is assumed to be uniform along the y-dimension of the active region.

By applying (4)-(5) to (2)-(3) and expressing the electric field in terms of the static potential ($E=-\nabla\varphi$), the system of equations (1)-(5) can be reduced to:

$$\nabla\left(\varepsilon_0\varepsilon_r\cdot\nabla\varphi\right)+q\cdot\left(p-n+N_D-N_A\right)=0 \tag{7}$$

$$\nabla\cdot\left(D_n\cdot\nabla n-\mu_n n\cdot\nabla\varphi\right)-R+G_n=0 \tag{8}$$

$$\nabla\cdot\left(D_p\cdot\nabla p+\mu_p p\cdot\nabla\varphi\right)-R+G_p=0 \tag{9}$$

Equations (7)-(9) are discretized by using the finite-difference method, where the Scharfetter-Gummel technique is applied to the dicretization of the carrier concentrations [6]. Special attention is focused on the carrier mobilities, since they depend on many factors, such as doping concentrations, electric field intensity and temperature. For details, the reader is referred to [6]. The resulting, non-linear, system of equations is solved for n, p and φ by using Newton's method. Once the carrier concentrations are obtained, the conductivity distribution is calculated by

$$\sigma=q\cdot\left(n\mu_n+p\mu_p\right) \tag{10}$$

B. Full Wave Analysis

The conductivity distribution along the TWPD's cross-section is used in the full wave simulation to obtain the microwave parameters of interest. Since some of the layers of the TWPD are up to 100 times thinner than others, the time step in a time-domain space-discretization technique would have to be very small, leading to large computation times. Therefore, a frequency-domain technique appears to be more suitable for the simulation of such structures.

In this project, the full-wave frequency-domain TLM (FDTLM) method [1], [2], which has been proven to be a reliable and a robust numerical tool for 2D and 3D field simulations has been chosen. In FDTLM, the computational domain is discretized by symmetrical condensed nodes, which represent a 3D transmission line network with 12 ports. The EM field is represented by a set of voltage waves traveling through the mesh along the propagation direction. The voltage waves are scattered at the centers of the nodes and phase-shifted to their ports. The scattering and phase-shift terms are calculated taking into account the material parameters at the location of each node. In our calculations, we use zero-reflection termination (ZRT) boundary conditions at the outer boundaries [2] to limit the computational space.

III. Results

To validate our approach, we have first analyzed the TWPD taken from [4]. The cross-section of the device is shown in Fig. 1. UD sections are unintentionally doped, and QW is the quantum well section. The optical waveguide, optimized for 1.06 μm wavelength, consists of the intrinsic (UD) layers sandwiched in between the p- and n-doped semiconductors. The width of the optical waveguide is 1.215μm. However, the absorption occurs only in the 15nm thick QW of InGaAs, while the other layers are transparent to light. As a result, the waveguide as a whole has a low optical absorption coefficient α_{abs} of 30 cm^{-1}, although InGaAs itself is a highly absorbing material for 1.06μm light. The advantage of such design is that the TWPD can operate under high illumination power without overheating. However, the length of the device must exceed 500 μm for 95% efficiency [4].

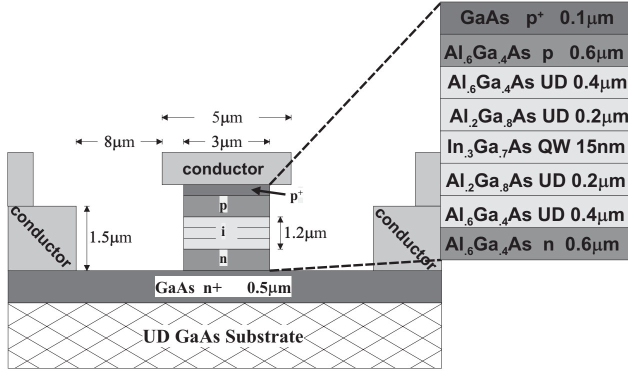

Fig. 1 Cross-section of the TWPD taken from [4].

A. Propagation Parameters and Characteristic Impedance

First, the TWPD is analyzed without the optical input signal. The obtained results are compared to those given in [4]. To operate this TWPD, a reverse bias voltage of 20 V is applied. A typical slow-wave behavior can be observed and is illustrated in the graphs of Fig. 2. It is evident that from the analysis presented here, the slow-wave factor (SWF) is much better predicted than with the equivalent circuit model. The SWF is very close to the optical index (3.2), meaning a very good match between the MW and optical velocities. The prediction of the microwave loss deviates from measurements. This is likely due to the fact that the exact doping concentrations of the n^+ and p^+ regions are not given in [4], and the estimated values may not be completely accurate. Since RF losses are very sensitive with respect to the conductivity (doping levels) of the layers, doping concentrations must be known to predict RF losses accurately.

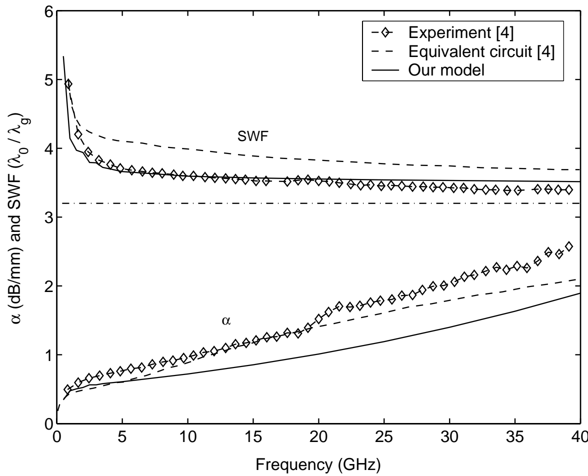

Fig. 2 RF loss and slow-wave factor of the TWPD.

When an optical signal is applied to the input of the photodetector, the photo generated carriers will increase the conductivity of the *intrinsic* region. Therefore, the propagation parameters of the microwave signal will change as well. Fig. 3 shows the propagation parameters of the microwave signal for different levels of the optical power. Both, the SWF and the attenuation constant increase with optical power. However, the attenuation constant is affected more strongly by the optical signal than the slow-wave factor. While the change of SWF (and thus the propagation velocity) is the largest at lower frequencies, RF losses seem to increase more at the higher frequencies. One should note that the TWPD is designed for optical powers up to 225 mW, where the effect on the propagation parameters will be even stronger.

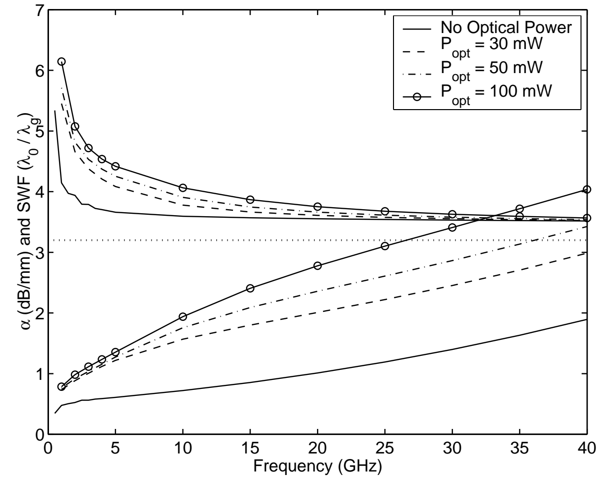

Fig. 3 RF propagation parameters of the TWPD for different levels of optical power.

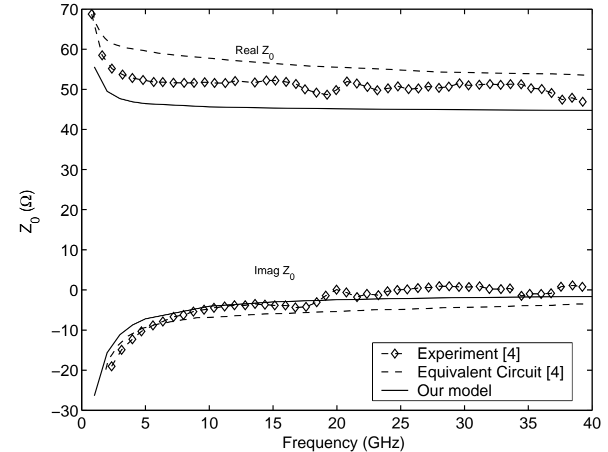

Fig. 4 Complex characteristic impedance of the TWPD for zero optical power.

Fig. 4 shows the real and imaginary parts of the characteristic impedance for zero optical power. While the predictions are somewhat lower for the real part of the

impedance, the imaginary part is in excellent agreement with the experiment. Again, the reason for the slight discrepancy is most likely a different doping level used in the real structure.

Also the complex characteristic impedance is calculated for different levels of the optical power, and is shown in Fig. 5. It is evident that with increasing optical power the real part of the impedance decreases, while the imaginary part approaches zero. Both, the real and the imaginary parts are affected more strongly at the lower frequency range.

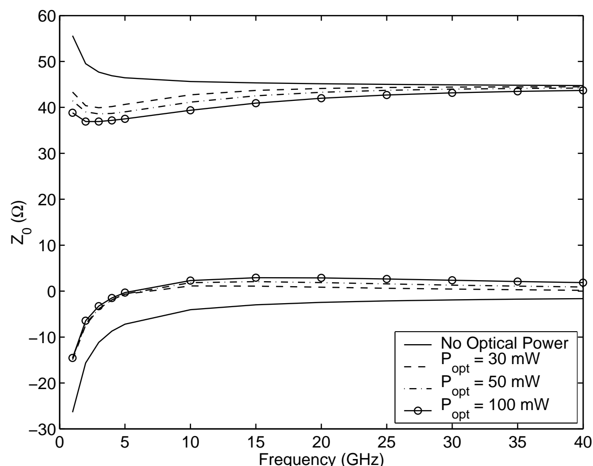

Fig. 5 Complex characteristic impedance of the TWPD for different levels of optical power.

B. S-parameter calculations

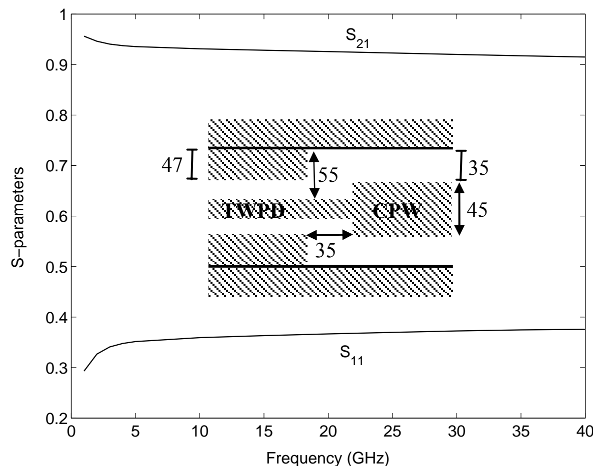

Fig. 6 S-parameters of the TWPD to CPW transition. All dimensions are in μm.

The interaction of the TWPD with the embedding microwave circuit is of great importance to ensure maximum RF power transfer. Fig. 6 shows first results for the transition between the TWPD and a CPW on GaAs substrate (undoped). The 35 μm long section between the TWPD and the CPW is built on undoped GaAs substrate and has the same shape and dimensions of the TWPD, except for the 55 μm wide gap. The S-parameters are calculated for the zero optical power case, because it is assumed that the optical signal will be absorbed by the time it reaches the interface. For this transition matching can not be achieved, and a considerable amount of power is reflected back into the TWPD.

IV. Conclusions

An efficient method for the rigorous analysis of TWPDs is presented. The conductivity distribution along the cross-section of the TWPD is found by a 2D drift-diffusion simulation of the structure. A full wave simulation is then performed to obtain the microwave parameters of interest. The method is used for 2D and 3D analyses of the TWPD from [4]. Simulation data obtained for the *zero optical* power case are in excellent agreement with experiments. The analysis is extended to include different optical power levels. The effect of the input light on the RF slow-wave factor and the characteristic impedance is more pronounced at lower RF frequencies, while the attenuation constant is affected more strongly at higher frequencies.

References

[1] H. Jin and R. Vahldieck, "The frequency-domain transmission line matrix method – a new concept," *IEEE Trans. Microwave Theory and Tech.*, vol. 40, pp. 2207-2218, December 1992.

[2] D. Pasalic, J. Bornemann, and R. Vahldieck, "Absorbing boundary conditions in the frequency-domain TLM method and their application to planar circuits," *IEEE Trans. Microwave Theory and Tech.*, vol 49, no. 8, pp. 1469-1476, August 2001.

[3] K. S. Giboney, M. J. Rodwell, J. E. Bowers, "Traveling-wave photodetector theory," *IEEE Trans. Microwave Theory and Tech.*, vol. MTT-45, no. 8, pp. 1310-1319, August 1997.

[4] V. M. Hietala, G. A. Vawter, T. M. Brennan, B. E. Hammons, "Traveling-wave photodetectors for high-power large-bandwidth applications," *IEEE Trans. Microwave Theory and Tech.*, vol. MTT-43, no. 9, pp. 2291-2298, September 1995.

[5] J-W. Shi and C.-K. Sun, "Design and analysis of long absorption-length traveling-wave photodetectors," *IEEE Journal of Light. Tech.*, vol. 18, no. 12, pp. 2176-2186, December 2000.

[6] S. Selberherr, *Analysis and Simulation of Semiconductor Devices*, Wien, New York: Springer-Verlag, 1984.